Title
Heat capacity (150–300 K) and anisotropic magnetic susceptibility (5–300 K) of single-crystal La2CuO4+x

Journal
Journal of Alloys and Compounds, 183(C)

ISSN
0925-8388

Authors
Miller, LL
Sun, K
Johnston, DC
et al.

Publication Date
1992-05-01

DOI
10.1016/0925-8388(92)90755-x

Journal of Alloys and Compounds, 183 (1992) 312–324
JALCOM 7018

Heat capacity (150–300 K) and anisotropic magnetic susceptibility (5–300 K) of single-crystal La_2CuO_{4+x}*

L. L. Miller, K. Sun and D. C. Johnston
Ames Laboratory–USDOE and Department of Physics and Astronomy, Iowa State University, Ames, IA 50011 (USA)

J. E. Schirber
Sandia National Laboratories, Albuquerque, NM 87185 (USA)

Z. Fisk
Los Alamos National Laboratory, Los Alamos, NM 87545 (USA)

(Received July 19, 1991)

Abstract

Heat capacity measurements from 150 to 300 K were carried out on a single crystal of La_2CuO_{4+x} synthesized by subjecting an La_2CuO_4 crystal to 3 kbar oxygen pressure at 575 °C. The data reveal three small (about 1%) anomalies at temperatures (T) of 206, 222 and 259 K. The first two are tentatively attributed to CuO inclusions in the crystal. The third is observed on warming, but not on cooling, and is attributed to the previously documented first-order transition from the orthorhombically distorted K_2NiF_4 structure to a low T mixture of nearly stoichiometric La_2CuO_4 and oxygen-rich superconducting La_2CuO_{4+y} ($y > x$). The size of the anomaly at 259 K is about one-seventh of that observed previously for a single crystal of La_2CuO_4 at the second-order tetragonal-to-orthorhombic phase transition temperature of about 530 K. Magnetization measurements from 5 to 300 K and from 50 G to 50 kG are also reported for the La_2CuO_{4+x} crystal. The normal state magnetic susceptibility $\chi(T)$ is quite anisotropic, with $\chi(T)$ for H perpendicular to the CuO_2 layers (χ_c) in good agreement with previous data on a different, but similarly prepared, crystal. The anisotropy in χ is nearly independent of T from 40 to 300 K and the magnitude of $\chi_c - \chi_{ab}$ per CuO_2 layer is very similar to that at high T in $YBa_2Cu_3O_{6.1}$, La_2CuO_4, $Sr_2CuO_2Cl_2$ and $La_{2-x}M_xCuO_4$ (M = Sr, Ba).

1. Introduction

The system La_2CuO_{4+x} exhibits a range of novel properties depending on the oxygen content $4+x$. The lowest oxygen content samples ($x \approx 0$) exhibit a second-order structural transition at a temperature $T_0 \approx 530$ K [1–4], become antiferromagnetically ordered below a Néel temperature $T_N \approx 300$ K

*Dedicated to Professor W. Bronger and Professor Ch. J. Raub on the occasions of their 60th birthdays.

0925-8388/92/$5.00

[4, 5] and are insulators as T goes to zero [6]. The transition from the high T tetragonal K_2NiF_4 structure at an orthorhombically distorted structure at T_0 results from tilting of the CuO_6 octahedra about the tetragonal (110) axis [3, 7]. The heat capacity jump at T_0 is $\Delta C_p(T_0) \approx 20$ mJ g^{-1} K^{-1} or about 5% of the lattice heat capacity at T_0 [8]. For a single crystal the C_p anomaly had a shape indicative of fluctuations in the orthorhombic order parameter near T_0 [8]. The transition at T_0 is evident in the powder magnetic susceptibility $\chi(T)$ via a distinct decrease in $d\chi/dT$ at T_0 upon cooling [9]. No anomalies were observed in $C_p(T)$ at $T_N = 304$ K for the above single crystal [8]. Only small effects are expected, because strong two-dimensional (2D) dynamic short-range antiferromagnetic (AF) order within the CuO_2 planes [10–14] causes the magnetic entropy at T_N to be only about 0.5% of the limiting high temperature value $R\ln 2$ [8]. A pronounced peak in $\chi(T)$ occurs at T_N [6, 15–20], originating as follows [18, 20–22]. Above T_N, weak ferromagnetic (FM) correlations build up within the CuO_2 layers with decreasing T below T_0, perpendicular to the instantaneous local axis of dynamic AF ordering. These FM correlations arise as a consequence of the orthorhombic distortion which introduces a Dzyaloshinsky–Moriya interaction $D \cdot (\mathbf{S}_i \times \mathbf{S}_j)$ into the intraplanar spin Hamiltonian below T_0 [22]. As the AF correlation length increases with decreasing T, the FM component within a correlated area increases in magnitude, tending towards a divergence near T_N. Below T_N the ferromagnetically canted components align perpendicular to the CuO_2 layers, with AF alignment in adjacent layers, resulting in the peak in $\chi(T)$ at T_N. This peak does not occur in the absence of the orthorhombic distortion, as verified for the tetragonal insulators $Sr_2CuO_2Cl_2$ [23] and $Ca_{0.85}Sr_{0.15}CuO_2$ [24] at their respective Néel temperatures of about 300 and 540 K. (For a recent review of the normal state magnetic susceptibilities of the La_2CuO_4-based compounds and the $YBa_2Cu_3O_{6+x}$ system see the article by Johnston [25].)

Subjecting La_2CuO_4 crystals to high (3 kbar) oxygen pressure at 500–600 °C induces bulk superconductivity below $T_c \approx 40$ K [26, 27]. Excess oxygen apparently enters the lattice as O_2 and an electron is transferred from Cu^{2+} to form a complicated oxygen complex and Cu^{3+} [28–30]. The superconductivity results from a first-order phase separation [27, 28, 31–34] of the La_2CuO_{4+x} below $T_s \approx 260$–280 K into an oxygen-rich superconducting composition, estimated to be $La_2CuO_{4.08}$, and nearly stoichiometric La_2CuO_4 with $T_N \approx 250$ K $\approx T_s$. The relative fractions of the two phases at 0 K are typically about 2:1 respectively [27, 28, 32]. This phase separation involves the bulk diffusion of atomic oxygen, showing that this diffusion is rapid even below room temperature. The T_0 value of the homogeneous sample above T_s is markedly suppressed from the value for La_2CuO_4 (530 K) to about 400 K $> T_s$ [27].

Herein we report $C_p(T)$ measurements from 150 to 300 K on a single crystal of La_2CuO_{4+x} which were carried out to search for a thermal anomaly at T_s for comparison with the results at T_0 for La_2CuO_4 [8] cited above. $\chi(T)$ measurements (40–300 K) with H parallel to c were carried out for

comparison with previous measurements [34] on a different crystal. Additional $\chi(T)$ measurements above 40 K with H perpendicular to c were done to determine the $\chi(T)$ anisotropy in the normal state. Finally, $\chi(T)$ data from 5 to 40 K for H both parallel and perpendicular to c were obtained to characterize the superconducting state below $T_c \approx 37$ K.

2. Experimental details

A single crystal of La_2CuO_4 of mass 72.8 mg was grown in a CuO flux as described previously [34]. The irregularly shaped crystal was annealed in an oxygen atmosphere at 3 kbar pressure and 575 °C for 12 h, followed by cooling to room temperature at a rate of about 100 °C min^{-1}. From previous work on similarly annealed crystals [28] the oxygen excess in the resulting La_2CuO_{4+x} crystal is estimated to be $x = 0.03$–0.04.

Heat capacity (C_p) data were obtained from 150 to 300 K using a Perkin–Elmer DSC-7 differential scanning calorimeter (DSC). The DSC was calibrated using pure indium metal. The calibration was checked by measuring $C_p(T)$ of pure colorless sapphire and comparing with high accuracy literature data [35]. This comparison showed that the accuracy of the DSC measurements of C_p is better than 8% for the 150–400 K temperature range. The precision of the measurements is better than 1% in this T range. Further calibration details can be found in ref. 8. $C_p(T)$ data for the La_2CuO_{4+x} crystal were obtained on both warming and cooling, using various temperature ramp rates from 2.5 to 80 K min^{-1}. The upper temperature limit of both the C_p measurements and the $\chi(T)$ measurements was 300 K, to avoid evolving the excess oxygen from the crystal which occurs at somewhat higher temperatures [30]. The DSC was cooled by liquid nitrogen and measurements were conducted after the DSC had reached a steady state using this coolant. The crystal was placed in a clean aluminum pan and the sample chamber was continuously purged with helium gas at a rate of 30 mL min^{-1}. The DSC was enclosed in a nitrogen-purged dry-box to avoid water condensation.

Magnetization (M) measurements of the La_2CuO_{4+x} crystal were carried out using a SQUID magnetometer (Quantum Design, Inc.). The crystal was mounted on a rigid sample holder, with H either parallel or perpendicular to the CuO_2 layers, using a small amount of GE 7031 varnish (which yielded a small diamagnetic contribution to the magnetization). Data were obtained from 5 to 300 K in applied magnetic fields (H) from 50 G to 50 kG in a low pressure helium atmosphere. Isothermal $M(H)$ data were taken from $H = 1$ to 50 kG at various temperatures. Before each $M(H)$ scan with $T < 100$ K, H was set to zero and the sample temperature allowed to equilibrate at 100 K before lowering T to the desired value and measuring the $M(H)$ data. Analysis of the $M(H)$ data revealed no evidence for the presence of either ferromagnetic or paramagnetic (*i.e.* with Curie-type $\chi(T)$) impurities.

3. Results and discussion

3.1. Heat capacity

A typical $C_p(T)$ data set for our La_2CuO_{4+x} crystal obtained on warming at 10 K min^{-1} is shown in Fig. 1. Several small features (peaks) are apparent in the data, marked by arrows in the figure. Although the size of these peaks is close to the resolution of the measurements, their size and the temperatures at which they occur were reproducible in different measurements. The peaks occur at $T_1 = 205$–210, $T_2 = 220$–225 and $T_3 = 260$–265 K for a T ramp rate of 10 K min^{-1}. While the three peaks can all be seen on warming, the peak at T_3 is missing from all data sets obtained on cooling, as illustrated in Fig. 2 for heating–cooling rates of ± 10 K min^{-1}. The peaks appear with a better signal-to-noise ratio using faster scanning rates, as shown in Fig. 1 where a rate of 40 K min^{-1} was used; as expected, because of temperature lag

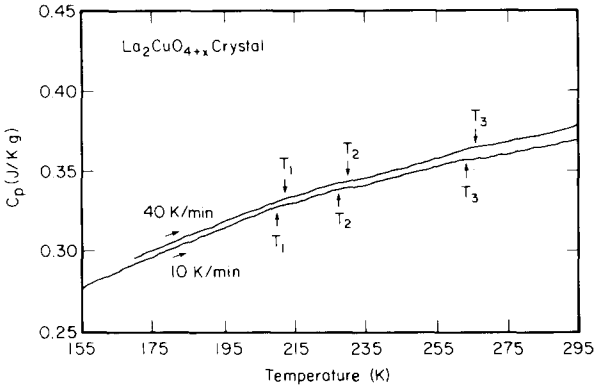

Fig. 1. Heat capacity C_p *vs.* temperature for single-crystal La_2CuO_{4+x}. The data were obtained using a DSC with heating rates of 10 and 40 K min^{-1} as shown.

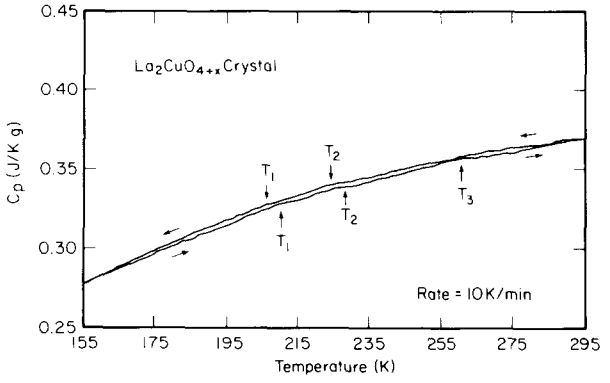

Fig. 2. Heat capacity C_p *vs.* temperature for single-crystal La_2CuO_{4+x}. The data were obtained using heating and cooling rates of 10 K min^{-1} as shown.

between the sample and thermometer, the apparent temperatures of the peaks are higher than obtained at 10 K min^{-1}. Many data sets as in Figs. 1 and 2 were obtained using heating rates of 10–80 K min^{-1}. Shown in Fig. 3 are the values of T_1, T_2 and T_3 obtained *vs.* the heating rate. By least-squares fitting the T_i data to straight lines and extrapolating to zero heating rate, the values in the absence of thermal lag between sample and thermometer were obtained: $T_1 = 205.6 \pm 1.1$, $T_2 = 221.6 \pm 2.2$ and $T_3 = 259.1 \pm 1.6$ K.

In an attempt to ascertain whether the three peaks in C_p depend on the thermal history of the sample, two additional types of experiments were carried out. In the first the crystal was first cooled to just above T_2, then heated to 300 K. It was found that the peak at T_3 was still always present in $C_p(T)$ obtained on warming but not on cooling. In the second the sample was first brought to thermal equilibrium at 250 K, then $C_p(T)$ data were obtained on cooling to 170 K and subsequent warming back to 250 K (*i.e.* without traversing the peak at T_3); the peaks at T_1 and T_2 were the same as observed above.

By examining the $C_p(T)$ data obtained on cooling and warming at the various temperature ramp rates, we could not identify any thermal hysteresis intrinsic to the transitions at T_1 and T_2. Of course, the transition at T_3 is hysteretic because no peak was observed in $C_p(T)$ on cooling, indicating that this transition is first order. The order of the other transitions at T_1 and T_2 could not be determined from analysis of the peak shapes in the present data owing to the small size of the respective C_p anomalies.

La_2CuO_{4+x} crystals synthesized using an oxygen pressure annealing schedule similar to that for our crystal undergo phase separation below room temperature, as noted in Section 1. We identify the peak in $C_p(T)$ at $T_3 = 259$ K observed on warming with this phase transition, which was deduced in ref. 34 to be first order from the thermal hysteresis found in resistance and $\chi(T)$ measurements, consistent with the thermal hysteresis we observe in $C_p(T)$. The reason why this transition is observed in our $C_p(T)$ data on

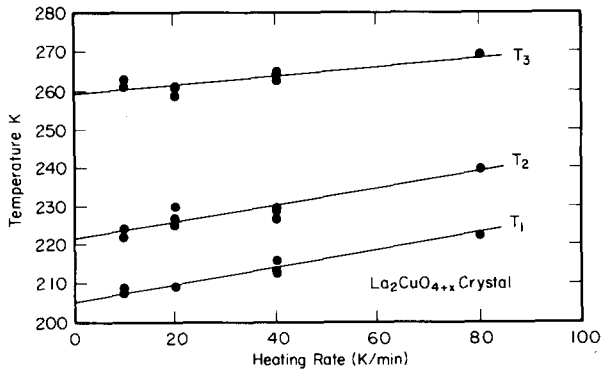

Fig. 3. Dependences of apparent temperatures of heat capacity peaks at T_1, T_2 and T_3, obtained using a DSC, *vs.* heating rate. Linear extrapolations to zero heating rate are shown.

warming but not on cooling is not clear. The peak is apparently broadened beyond our resolution during cooling. The $\chi(T)$ data below (taken on warming) are consistent with the phase transition occurring at $T_s = T_3$. An expanded plot of the 10 K min^{-1} ramp rate data of Fig. 1 in the vicinity of T_3 is shown in Fig. 4. The size of the anomaly may be characterized by the heat capacity jump at T_3 shown in the figure, $\Delta C_p(T_3) = 3$ mJ g^{-1} K^{-1}, which is about one-seventh of that seen [8] in La_2CuO_4 at $T_0 = 530$ K.

The peaks in $C_p(T)$ at T_1 and T_2 are most likely not associated with the bulk phase transition in La_2CuO_{4+x} at T_3, since the former peaks occur independently of whether the peak at T_3 is observed on warming and cooling. We tentatively attribute the peaks at T_1 and T_2 to phase transitions within CuO inclusions in the La_2CuO_{4+x} crystal, from the following considerations. For a sintered and annealed polycrystalline CuO sample, $C_p(T)$ measurements made with our DSC under the same operating conditions showed two transitions between 200 and 230 K [8]. A second-order transition was observed at $T_N = 225.0(2)$ K associated with long-range incommensurate AF order. A first-order transition occurred at $T_m = 209.5(2)$ K arising from a commensurate-to-incommensurate AF transition on warming. We therefore identify T_1 with T_m and T_2 with T_N. Comparing the size of the anomalies at T_1 and T_2 with those at T_m and T_N in the pure CuO sample, we estimate that our La_2CuO_{4+x} crystal contains about 4 wt.% of CuO inclusions. These inclusions presumably originate from the CuO flux during crystal growth.

3.2. Magnetization measurements

The zero-field-cooled (ZFC) and field-cooled (FC) susceptibility data ($\chi(T) \equiv M(T)/H$) below 50 K for $H = 50$ G are shown in Figs. 5(a) and 5(b) respectively. In each figure the data for H parallel (χ_{ab}) and perpendicular (χ_c) to the CuO_2 planes are shown. All data sets were obtained on warming from 5 K. The quantity on the ordinates is the (dimensionless c.g.s.) volume susceptibility χ_v normalized by the negative of the value ($-1/4\pi$) expected

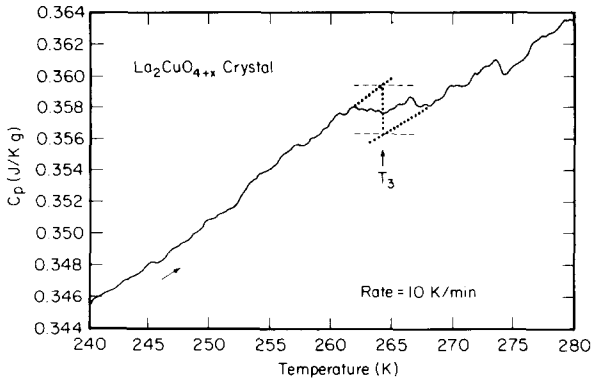

Fig. 4. Expanded plot near transition at T_3 of heat capacity C_p *vs.* temperature for single-crystal La_2CuO_{4+x}. The data were obtained using a DSC at a heating rate of 10 K min^{-1}. The construction for characterizing the size of the anomaly at the apparent T_3 is shown.

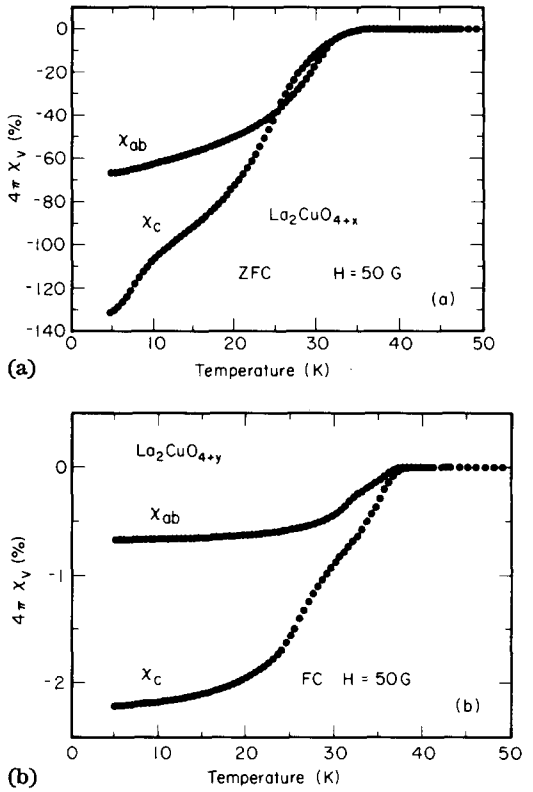

Fig. 5. Volume magnetic susceptibility χ_v *vs.* temperature for single-crystal La_2CuO_{4+x} below 50 K. The applied $H=50$ G was either parallel to the CuO_2 planes (χ_{ab}) or perpendicular to them (χ_c). The data were obtained upon warming from 5 K either (a) after cooling to 5 K in zero applied field (ZFC) or (b) after cooling to 5 K in the field of 50 G (FC).

for perfect diamagnetism. Demagnetization effects are not taken into account in Fig. 5 because of the irregular shape of the crystal. The ZFC data in Fig. 5(a) indicate that a large fraction (at least half) of the crystal exhibits bulk superconductivity at 5 K. In contrast, the FC Meissner effect $\chi(T)$ data in Fig. 5(b) are smaller in magnitude by factors of about 60–100. This discrepancy suggests either that flux pinning is strong below T_c or that only a small fraction (on the order of 1%) of the crystal volume exhibits bulk superconductivity. Quantitative analyses of neutron diffraction [27], muon spin rotation (μSR) [32] and ^{139}La nuclear quadrupole resonance (NQR) [33] experiments on similar samples indicate that the first interpretation is the correct one. Strong flux pinning might be expected because of the fine-grained macroscopic phase segregation occurring below $T_s=260$ K (see below).

Multiple inflections in the FC $\chi_c(T)$ data at 9 and 25 K and in the ZFC data at 26 and 35 K for $\chi_c(T)$ and at 31 and 35 K for $\chi_{ab}(T)$ suggest multiple superconducting transitions. However, the lower inflection temperatures for

the respective measurements are not the same and therefore most likely are manifestations of temperature-dependent flux-pinning effects. The temperatures corresponding to selected points on the transition curves in Fig. 5 are listed in Table 1, where corresponding temperatures for data at $H = 10$ kG (not shown) are included. Also listed are the superconducting onset temperatures obtained by the intersection of straight line extrapolations of the data above 40 K and the first linear region below the first detectable onset of diamagnetism.

The susceptibilities from 40 to 300 K with $H = 10$ kG parallel (χ_{ab}) and perpendicular (χ_c) to the CuO_2 planes are shown in Fig. 6(a); the data were taken on warming after zero-field cooling to 5 K and applying the field at that T. From the figure the high temperature onset of the phase separation transition is at 260–270 K. The maximum negative slope in both $\chi_c(T)$ and $\chi_{ab}(T)$ occurs at $T_s = 255$–260 K. The temperature of the peak in the above $C_p(T)$ measurements at $T_3 = 259 \pm 1.6$ K is equal (within the errors) to T_s, consistent with assigning this peak in $C_p(T)$ to the phase separation transition. However, the presence of 4 wt.% CuO inclusions in our La_2CuO_{4+x} crystal, as deduced from anomalies at $T_1 = 206$ and $T_2 = 222$ K in the $C_p(T)$ measurements, is not evident in the $\chi(T)$ data in Fig. 6(a) (or Fig. 6(b) below). The value of T_s is in agreement with values determined from $\chi(T)$ [34], resistivity [34] and ^{139}La NQR [33] measurements of similarly prepared crystals. The $\chi_c(T)$ data are nearly identical to those taken previously on warming for a different La_2CuO_{4+x} crystal synthesized under the same conditions as our crystal [34]. Measurements of the hysteretic behavior of $\chi(T)$, observed in $\chi_c(T)$ in ref. 34 upon warming and cooling, were not made in the present work.

TABLE 1

Superconducting transition values for single-crystal La_2CuO_{4+x}. The '$T-H$ process' refers to whether the crystal was cooled to 5 K in zero applied field prior to measurement (ZFC) or whether the indicated field was applied above T_c (FC); all data were obtained upon increasing the temperature from 5 K. The transition temperatures indicated are the onset temperature (see text) and the temperatures at which the magnetization attained 10% and 50% of its maximum diamagnetic value at 5 K. χ_v is the dimensionless c.g.s. volume susceptibility (χ defined as M/H); the last column is normalized to the value expected for perfect diamagnetism

Data set	Applied field	T–H process	Transition temperature (K)		$4\pi\chi$(5 K) (%)
			10%	50%	
χ_{ab}	10 kG	ZFC	16	25	−0.5
χ_c	10 kG	ZFC	25	16	−30.2
χ_{ab}	50 G	ZFC	32	26	−66.8
χ_{ab}	50 G	FC	35	31	−0.7
χ_c	50 G	ZFC	29	21	−132.0
χ_c	50 G	FC	35	28	−2.2

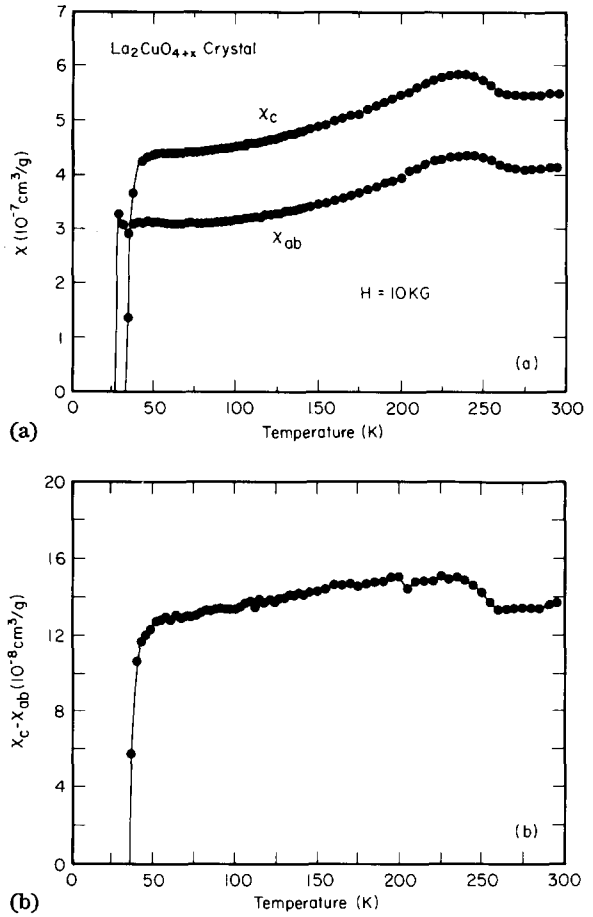

Fig. 6. (a) Magnetic susceptibility χ *vs.* temperature for single-crystal La_2CuO_{4+x}. The applied field of 10 kG was either parallel (χ_{ab}) or perpendicular (χ_c) to the CuO_2 planes. The data were obtained on warming after cooling to 5 K in zero applied field. (b) Magnetic susceptibility anisotropy $\Delta\chi$, defined as $\chi_c - \chi_{ab}$, *vs.* temperature above about 40 K, computed from (a).

A nearly temperature-independent anisotropy $\Delta\chi \equiv \chi_c - \chi_{ab}$ is observed in Fig. 6(a) and is plotted *vs.* T in Fig. 6(b). At 290 K, $\chi_c = 5.51 \times 10^{-7}$, $\chi_{ab} = 4.12 \times 10^{-7}$ and $\Delta\chi = 1.39 \times 10^{-7}$ cm^3 g^{-1}. The lattice transformation causes $\Delta\chi$ to increase by about 10% below T_s; $\Delta\chi$ then returns to the value above T_s around 100 K. The negative curvatures in $\chi_c(T)$ and $\Delta\chi(T)$ below about 60 K in Fig. 6 most likely arise primarily from (anisotropic) superconducting fluctuation diamagnetism above T_c, as has been observed and documented previously for several of the other superconducting cuprates between T_c and $2T_c$ [9, 36–43].

The μSR measurements on a powder sample of La_2CuO_{4+x} revealed AF ordering below $T_N = 250$ K (with roughly equal amounts of the oxygen-rich superconducting phase and the antiferromagnetically ordered La_2CuO_4 phase

at low T) [32]. The phase separation temperature in our La_2CuO_{4+x} crystal is $T_s = 260$ K. Thus T_N and T_s are expected to be identical or close to each other. The La_2CuO_4 phase is expected to exhibit a pronounced peak in $\chi(T)$ at T_N as discussed in Section 1, whereas the data in Fig. 6(a) show only a shallow peak at about 240 K. We speculate that this discrepancy arises from smearing of the peak resulting from a fine-grained morphology of the phase mixture below T_s and/or to associated lattice strain below T_s [44]. Additionally, the proximity of T_s and T_N makes extraction of the individual influences of phase separation and AF ordering from $\chi(T)$ difficult.

Both $\chi_c(T)$ and $\chi_{ab}(T)$ in Fig. 6(a) increase slowly with T above $T_s = 260$ K. This is similar to the $\chi(T)$ behavior above T_c or T_N for other superconducting cuprates and insulating parent compounds not containing magnetic ions other than Cu^{2+} and is believed to reflect the occurrence of dynamic 2D short-range AF ordering of the (nearly) localized Cu^{2+} spin-$\frac{1}{2}$ magnetic moments resulting from strong ($J \approx 1500$ K) AF exchange coupling between these ions [25]. In support of this interpretation the high temperature anisotropy ($\Delta\chi$) in Fig. 6(b) is about the same per CuO_2 layer as in $YBa_2Cu_3O_{6.1}$ [45] and in other K_2NiF_4-type compounds such as La_2CuO_4 [8], $Sr_2CuO_2Cl_2$ [23] and $La_{2-x}(Sr,Ba)_xCuO_4$ [18]; this suggests that the local electronic states and state occupations in the vicinity of the Cu^{2+} ions are similar in these compounds. Indeed, the anisotropy in both the insulating and superconducting cuprates is believed to arise primarily from the anisotropic Van Vleck paramagnetic orbital susceptibility of the (nearly) localized Cu^{2+} ions, with a small additional anisotropic spin susceptibility contribution coming from an anisotropic spectroscopic splitting factor (g) of these ions [40, 41, 45–48].

4. Summary and concluding remarks

Heat capacity (C_p) measurements between 150 and 300 K of single-crystal La_2CuO_{4+x} revealed small (about 1%) thermal anomalies at $T_1 = 206$, $T_2 = 222$ and $T_3 = 259$ K. The first two transitions are tentatively ascribed to about 4 wt.% CuO inclusions in the crystal. The anomaly at T_3 is attributed to the previously documented [27, 28, 31–34] first-order transition from the homogeneous orthorhombically distorted La_2CuO_{4+x} phase above $T_s = T_3$ to the low T phase-separated mixture of nearly stoichiometric La_2CuO_4 with $T_N \approx 250$ K [32] and oxygen-rich La_2CuO_{4+y}; x and y were found in previous work to be about 0.03–0.04 and 0.08 respectively [23]. The size of the C_p anomaly at T_s, $\Delta C_p \approx 3$ mJ g^{-1} K^{-1}, is about one-seventh of that found previously [8] at the second-order tetragonal-to-orthorhombic phase transition temperature $T_0 \approx 530$ K in an La_2CuO_4 crystal with $T_N = 304$ K. The first-order character of the transition at T_s is manifested in $C_p(T)$ by the appearance of an anomaly on heating but not on cooling, although no explicit evidence for a latent heat at T_s was observed.

The similarity of our La_2CuO_{4+x} crystal and a different one on which extensive magnetic susceptibility ($\chi(T)$) and transport measurements were carried out previously [34] was verified here via magnetization measurements. The χ data obtained on heating from 40 to 300 K with the applied field H perpendicular to the CuO_2 planes ($\chi_c(T)$) are essentially identical to those reported previously [34], including the data in the important T region near T_s. The χ data with H parallel to the CuO_2 planes ($\chi_{ab}(T)$) were also measured with increasing T. The anisotropy $\Delta\chi$, defined as $\chi_c - \chi_{ab}$, was found to be nearly independent of T from 40 to 300 K, although a small (10%) increase in $\Delta\chi$ was observed below T_s. Superconducting fluctuation diamagnetism between T_c and about 60 K was apparent in the $\chi(T)$ data.

The interpretation of the $\chi_{ab}(T)$ and $\chi_c(T)$ anomalies in our crystal below T_s is ambiguous at present. μSR experiments on a powder sample of La_2CuO_{4+x} (annealed similarly under oxygen pressure) showed that the $T_N \approx 250$ K. However, the anisotropy and size of the anomalies we see in $\chi_c(T)$ and $\chi_{ab}(T)$ near 250 K are different than in single-crystal La_2CuO_4 with $T_N \approx 250$ K [32]. The apparent near coincidence of T_s and T_N makes extraction of the individual magnetic ordering and chemical–crystallographic contributions to the $\chi(T)$ anomalies problematic; further complications arise from possible size effects and strain in the phase-separated mixture below T_s. We hope to address these issues in part through future magnetic and crystallographic neutron diffraction measurements on the present La_2CuO_{4+x} crystal.

Finally, from the above discussion and that in Section 1, one would infer that (i) the most oxygen-rich composition of the antiferromagnetically ordered La_2CuO_4 phase has a minimum T_N of about 250 K. This is to be contrasted with (ii) the observations that T_N values as low as 50 K are seen by magnetic neutron diffraction for some single crystals [18] and that annealing at 500 °C in only modest (100 bar) oxygen pressures is sufficient to drive T_N from 290 K to near 0 K in certain powder samples without inducing any trace of superconductivity above 4 K [6, 9]; the increase in oxygen content in the latter case is about 0.03 [9]. We speculate that the reason for the contradictory results (i) and (ii) is that some La_2CuO_z samples contain cation vacancies, up to about 1%, on the lanthanum and/or copper sites. For example, for 1% La vacancies the oxygen composition giving all Cu^{2+} ions and presumably the highest T_N would be $La_{1.98}CuO_{3.97}$. By increasing the oxygen content to 4.00, T_N might be driven to zero without, however, inducing phase separation and superconductivity. These ideas are currently under investigation.

Acknowledgments

One of us (D.C.J.) is grateful for the generous hospitality of Dr. Takehiko Matsumoto and the National Research Institute for Metals in Tokyo, Japan, where part of this paper was written. Ames Laboratory is operated for the US Department of Energy by Iowa State University under Contract No.

W-7405-Eng-82. The work at Ames was supported by the Director for Energy Research, Office of Basic Energy Sciences. The work at Sandia National Laboratory was supported by the US Department of Energy under Contract DE-AC04-76DP00789. The work at Los Alamos was performed under the auspices of the US Department of Energy, Office of Basic Energy Science, Division of Materials Science.

References

1 P. Lehuédé and M. Daire, *C.R. Acad. Sci. (Paris), 276* (1973) C1011.
2 J. M. Longo and P. M. Raccah, *J. Solid State Chem., 6* (1973) 526.
3 B. Grande, Hk. Müller-Buschbaum and M. Schweizer, *Z. anorg. allg. Chem., 428* (1977) 120.
4 D. Vaknin, S. K. Sinha, D. E. Moncton, D. C. Johnston, J. M. Newsam, C. R. Safinya and H. E. King Jr., *Phys. Rev. Lett., 58* (1987) 2802.
5 S. Mitsuda, G. Shirane, S. K. Sinha, D. C. Johnston, M. S. Alvarez, D. Vaknin and D. E. Moncton, *Phys. Rev. B, 36* (1987) 822.
6 D. C. Johnston, J. P. Stokes, D. P. Goshorn and J. T. Lewandowski, *Phys. Rev. B, 36* (1987) 4007.
7 J. D. Jorgensen, H.-B. Schüttler, D. G. Hinks, D. W. Capone II, K. Zhang, M. B. Brodsky and D. J. Scalapino, *Phys. Rev. Lett., 58* (1987) 1024.
8 K. Sun, J. H. Cho, F. C. Chou, W. C. Lee, L. L. Miller, D. C. Johnston, Y. Hidaka and T. Murakami, *Phys. Rev. B, 43* (1991) 239.
9 D. C. Johnston, S. K. Sinha, A. J. Jacobson and J. M. Newsam, *Physica C, 153–155* (1988) 572.
10 G. Shirane, Y. Endoh, R. J. Birgeneau, M. A. Kastner, Y. Hidaka, M. Oda, M. Suzuki and T. Murakami, *Phys. Rev. Lett., 59* (1987) 1613.
11 Y. Endoh, K. Yamada, R. J. Birgeneau, D. R. Gabbe, H. P. Jenssen, M. A. Kastner, C. J. Peters, P. J. Picone, T. R. Thurston, J. M. Tranquada, G. Shirane, Y. Hidaka, M. Oda, Y. Enomoto, M. Suzuki and T. Murakami, *Phys. Rev. B, 37* (1988) 7443.
12 K. Yamada, K. Kakurai, Y. Endoh, T. R. Thurston, M. A. Kastner, R. J. Birgeneau, G. Shirane, Y. Hidaka and T. Murakami, *Phys. Rev. B, 40* (1989) 4557.
13 G. Aeppli, S. M. Hayden, H. A. Mook, Z. Fisk, S-W. Cheong, D. Rytz, J. P. Remeika, G. P. Espinosa and A. S. Cooper, *Phys. Rev. Lett., 62* (1989) 2052.
14 S. M. Hayden, G. Aeppli, H. A. Mook, S-W. Cheong and Z. Fisk, *Phys. Rev. B, 42* (1990) 10220.
15 S. Uchida, H. Takagi, H. Yanagisawa, K. Kishio, K. Kitazawa, K. Fueki and S. Tanaka, *Jpn. J. Appl. Phys., 26* (1987) L445.
16 R. L. Greene, H. Maletta, T. S. Plaskett, J. G. Bednorz and K. A. Müller, *Solid State Commun., 63* (1987) 379.
17 K. Fukuda, M. Sato, S. Shamoto, M. Onoda and S. Hosoya, *Solid State Commun., 63* (1987) 811.
18 K. Fukuda, S. Shamoto, M. Sato and K. Oka, *Solid State Commun., 65* (1988) 1323, and references cited therein.
19 S.-W. Cheong, Z. Fisk, J. O. Willis, S. E. Brown, J. D. Thompson, J. P. Remeika, A. S. Cooper, R. M. Aikin, D. Schiferl and G. Gruner, *Solid State Commun., 65* (1988) 111.
20 S.-W. Cheong, J. D. Thompson, Z. Fisk and G. Gruner, *Solid State Commun., 66* (1988) 1019.
21 S.-W. Cheong, J. D. Thompson and Z. Fisk, *Phys. Rev. B, 39* (1989) 4395.
22 T. Thio, T. R. Thurston, N. W. Preyer, P. J. Picone, M. A. Kastner, H. P. Jenssen, D. R. Gabbe, C. Y. Chen, R. J. Birgeneau and A. Aharony, *Phys. Rev. B, 38* (1988) 905.

23 D. Vaknin, S. K. Sinha, C. Stassis, L. L. Miller and D. C. Johnston, *Phys. Rev. B, 41* (1990) 1926.
24 D. Vaknin, E. Caignol, P. K. Davies, J. E. Fischer, D. C. Johnston and D. P. Goshorn, *Phys. Rev. B, 39* (1989) 9122.
25 D. C. Johnston, *J. Magn. Magn. Mater., 100* (1991) 218.
Z. Fisk, S.-W. Cheong and D. C. Johnston, *Mater. Res. Soc. Bull., 14* (1989) 33.
S.-W. Cheong, J. D. Thompson and Z. Fisk, *Physica C, 158* (1989) 109.
26 J. Beille, R. Cabanel, C. Chaillout, B. Chevalier, G. Demazeau, F. Deslandes, J. Etourneau, P. Lejay, C. Michel, J. Provost, B. Raveau, A. Sulpice, J.-L. Tholence and R. Tournier, *C. R. Acad. Sci. (Paris), 304* (1987) 1097.
27 J. D. Jorgensen, B. Dabrowski, S. Pei, D. G. Hinks, L. Soderholm, B. Morosin, J. E. Schirber, E. L. Venturini and D. S. Ginley, *Phys. Rev. B, 38* (1988) 11337, and references cited therein.
28 C. Chaillout, S.-W. Cheong, Z. Fisk, M. S. Lehmann, M. Marezio, B. Morosin and J. E. Schirber, *Physica C, 158* (1989) 184.
29 K. F. McCarty, J. E. Schirber, S.-W. Cheong and Z. Fisk, *Phys. Rev. B, 43* (1991) 7883.
30 J. E. Schirber, B. Morosin, R. M. Merrill, P. F. Hlava, E. L. Venturini, J. F. Kwak, P. J. Nigrey, R. J. Baughman and D. S. Ginley, *Physica C, 152* (1988) 121.
31 P. Zolliker, D. E. Cox, J. B. Parise, E. M. McCarron III and W. E. Farneth, *Phys. Rev. B, 42* (1990) 6332.
32 E. J. Ansaldo, J. H. Brewer, T. M. Riseman, J. E. Schirber, E. L. Venturini, B. Morosin, D. S. Ginley and B. Sternlieb, *Phys. Rev. B, 40* (1989) 2555.
33 P. C. Hammel, A. P. Reyes, Z. Fisk, M. Takigawa, S.-W. Cheong, R. H. Heffner, J. D. Thompson and J. E. Schirber, *Phys. Rev. B, 42* (1990) 6781.
34 M. F. Hundley, J. D. Thompson, S.-W. Cheong, Z. Fisk and J. E. Schirber, *Phys. Rev. B, 41* (1990) 4062.
35 G. T. Furakawa, T. B. Douglas, R. E. McCloskey and D. C. Ginnings, *J. Res. Natl. Bur. Stand., 57* (1956) 67.
36 P. P. Freitas, C. C. Tsuei and T. S. Plaskett, *Phys. Rev. B, 36* (1987) 833.
37 T. R. McGuire, T. R. Dinger, P. J. P. Freitas, W. J. Gallagher, T. S. Plaskett, R. L. Sandstrom and T. M. Shaw, *Phys. Rev. B, 36* (1987) 4032.
38 K. Kanoda, T. Kawagoe, M. Hasumi, T. Takahashi, S. Kagoshima and T. Mizoguchi, *J. Phys. Soc. Jpn., 57* (1988) 1554.
K. Kanoda, T. Takahashi, T. Kawagoe, T. Mizoguchi, M. Hasumi and S. Kagoshima, *Physica C, 153–155* (1988) 749.
39 W. C. Lee, R. A. Klemm and D. C. Johnston, *Phys. Rev. Lett., 63* (1989) 1012.
40 W. C. Lee and D. C. Johnston, *Phys. Rev. B, 41* (1990) 1904.
41 D. C. Johnston and J. H. Cho, *Phys. Rev. B, 42* (1990) 8710.
42 W. C. Lee, J. H. Cho and D. C. Johnston, *Phys. Rev. B, 43* (1991) 457.
43 M. Miljak, G. Collin and A. Hamzić, *J. Magn. Magn. Mater., 76–77* (1988) 609.
M. Miljak, G. Collin, A. Hamzić and V. Zlatić, *Europhys. Lett., 9* (1989) 723.
M. Miljak, V. Zlatic, I. Kos, I. Aviani, A. Hamzić and G. Collin, *Phys. Rev. B, 42* (1990) 10742.
44 A. Sulpice, P. LeJay, R. Tournier, B. Chevalier, G. Demazeau and J. Etourneau, *Physica B, 165–166* (1990) 1157, and references cited therein.
45 Y. Yamaguchi, M. Tokumoto, S. Waki, Y. Nakagawa and Y. Kimura, *J. Phys. Soc. Jpn., 58* (1989) 2256.
46 M. Takigawa, P. C. Hammel, R. H. Heffner, Z. Fisk, J. L. Smith and R. B. Schwarz, *Phys. Rev. B, 39* (1989) 300.
47 S. E. Barrett, D. J. Durand, C. H. Pennington, C. P. Slichter, T. A. Friedmann, J. P. Rice and D. M. Ginsberg, *Phys. Rev. B, 41* (1990) 6283.
48 R. E. Walstedt and W. W. Warren Jr., *Science, 248* (1990) 1082.